Estimating the Local Mean Voltage of a Radio Signal in a Mobile Channel

Robert Johnk
Institute for Telecommunication Sciences (NTIA/ITS)
U.S. Department of Commerce Boulder Laboratories
Boulder, Colorado 80305, USA
Contact: rjohnk@ntia.gov

John J. Lemmon
Formerly with the Institute for Telecommunication Sciences
Contact: johnjlemmon@gmail.com

***Abstract*— This paper examines the estimation of the local mean voltage of a radio signal in a Rayleigh fast-fading environment. We focus on the statistical uncertainties of local voltage averages obtained by both integrating the voltage envelope of a specified spatial interval and averaging over a set of discrete spatial samples. We derive new analytical expressions of the variances of both discrete and continuous averaging for selected spatial intervals. We also give recommendations for averaging intervals and sample spacing to achieve a ±1 dB spreading factor. We provide important new results for the variance of discrete averaging with new insight gained on separations required for uncorrelated samples. One significant finding of this work is that criteria in the published literature are incorrect and underestimate the variance. We support these findings with an experimental validation of our variance expressions using laboratory fading simulator measurements and sample statistics.**

Keywords—Autocorrelation, Continuous Average, Correlation, Coverage Factor, CW Channel sounder, Discrete Average, Ensemble Average, Fast Fading, IQ Envelope, Local Mean, Lee 40-Wavelength Criterion, Path Loss, Propagation, Rayleigh, Sampling, Standard Deviation, Spreading Factor, Time Series, Variance, Vector Signal Analyzer.

I. Introduction

The Institute for Telecommunication Sciences (ITS) has developed and deployed a continuous-wave (CW) channel sounding system to measure radio channel properties [1]. This system has been deployed in a wide variety of outdoor clutter environments around the United States, ranging from open rural to dense urban environments [2]. The system transmits a CW signal from a fixed location to a receiver located in a van. The van is driven over prescribed routes and measures the received signal for the duration of the tests. The signal is received by a vector signal analyzer (VSA), which down-converts the signal to a baseband IQ data stream. After a drive test, the IQ samples are transferred to a computer and post processed to obtain useful propagation parameters such as path loss and fast-fading parameters.

One key element used in post processing of measured data to obtain path loss is window averaging. This process smooths the data and enables meaningful estimates of the local mean voltage. The local mean voltage is converted into power, which, in turn, is used to compute path loss. Two types of window averaging are described: continuous-time and discrete-time. The analysis and results that are presented here are applicable to non-line-of-sight (NLOS) Rayleigh, fast fading channels with a distribution of scatterers that results in a Jake's power spectrum [3].

II. Continuous and Discrete Windowed Averaging

Fig. 1 depicts a van with an onboard receiver that is recording IQ voltage data with an averaging interval of spatial extent $2L$ meters; λ is the wavelength in meters at the frequency of operation. This averaging interval is centered on a receiving antenna location on the roof of the van, and it extends $\pm L$ meters along the axis of travel.

The centered, rectangular averaging window that is used to process the received IQ envelope data, for both continuous and discrete-sampled data, is shown in Fig. 2. For the continuous-time case the complex baseband IQ signal can be written as

$$s(t) = r(t)e^{i\varphi(t)}, \tag{1}$$

where $r(t)$ and $\varphi(t)$ are the envelope and phase of the signal, respectively. An estimate of the local mean $\hat{m}$ at a location x can be obtained by averaging the IQ envelope *r(y)* over a distance $2L$ from *x-L to x+L*:

$$\hat{m}(x) = \frac{1}{2L}\int_{x-L}^{x+L} r(y)dy. \tag{2}$$

For a non-line-of sight channel with a uniform distribution of scatterers around a receiving location, the probability density

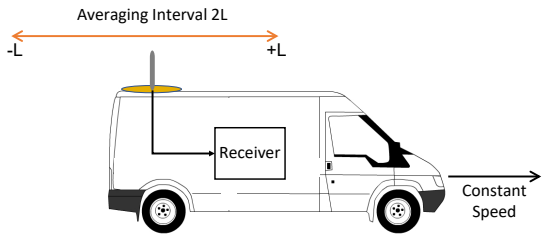

Fig. 1. A van collecting mobile channel data from a CW transmitter, traveling at a constant speed. The averaging interval 2L is centered on the receiving antenna.

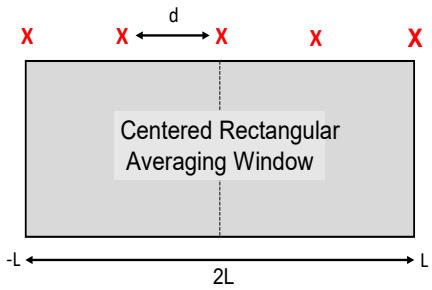

Fig. 2. Rectangular window used to smooth the received IQ voltage envelope. This window is used for either continuous waveforms or discrete data with a sample spacing of *d* (denoted by the red x's).

function of the received voltage envelope *r(t)* is a Rayleigh distributed random variable given by

$$p(r) = \frac{r}{b^2}\exp\left(-\frac{r^2}{2b^2}\right), \tag{3}$$

where $r \geq 0$ and b is a parameter with the dimensions of *r(t)* (volts in this case). The mean of (3) is given by

$$m_r = \langle r \rangle = \int_0^\infty r p(r) dr = \sqrt{\frac{\pi}{2}} b \tag{4}$$

where $\langle \cdot \rangle$ denotes the usual expectation operator E{}[4]. The variance of (3) is

$$\sigma_r^2 = \int_0^\infty r^2\, p(r) dr - m_r^2 = \left(2 - \frac{\pi}{2}\right) b^2. \tag{5}$$

Applying (3) and (4) to (2) and interchanging the order of integration and the expectation obtains the local mean

$$\langle \hat{m}(x) \rangle = \frac{1}{2L}\int_{x-L}^{x+L} \langle r(y) \rangle dy = \langle r(y) \rangle = \sqrt{\frac{\pi}{2}}\, b, \tag{6}$$

which is the same as the mean of the governing Rayleigh distribution of the voltage envelope *r(t)*.

In the past [5], continuous averaging was used to measure the local mean voltage and power. However, in more modern measurement systems, the local mean voltage is estimated by averaging a finite number of discrete samples from a digitizing receiver like a VSA. The red x's in Fig. 2 denote the location of uniformly spaced, discrete samples within the $2L$ averaging interval, spaced *d* meters apart. For *N* samples, the spacing is

$$d = \frac{2L}{(N-1)}. \tag{7}$$

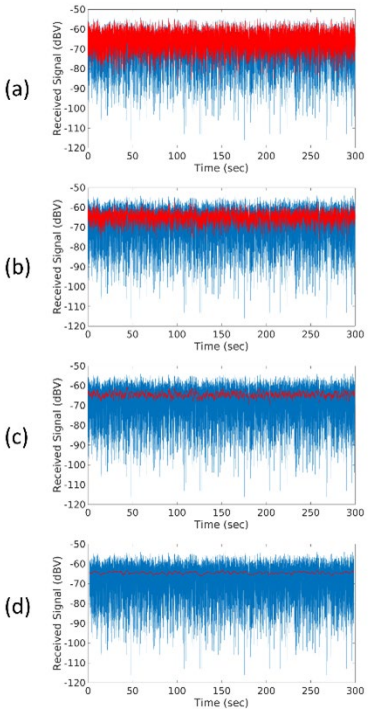

Fig. 3. Rayleigh faded IQ envelope (blue traces) and local mean (red traces). The window widths used are: (a) 0.25 λ, (b) 1 λ, (c) 6 λ, (d) 60 λ.

The estimated local mean using *N* discrete samples at a sequence of spatial locations x_i uniformly separated by a distance *d* is

$$\hat{m} = \frac{1}{N}\sum_{i=1}^{N} r_i\,, \tag{8}$$

where $r_i \equiv r(x_i)$. Applying the expectation operator $\langle \cdot \rangle$ to (8) and interchanging the order of summation and the expectation yields

$$\langle \hat{m} \rangle = \frac{1}{N}\sum_{i=1}^{N} \langle r_i \rangle = \sqrt{\frac{\pi}{2}} \mathrm{b} = m_r\,. \tag{9}$$

The ensemble average (9) of the discrete sampled measurements, once again, equals the mean of the governing Rayleigh distribution. While continuous signal acquisition and averaging is no longer used in propagation measurements, it does serve as a useful benchmark for discrete channel sampling.

Variance and Spread of the local mean

Fig. 3 shows the impact of window averaging. The IQ data were obtained from benchtop measurements using a mobile channel simulator. The channel simulator was configured to generate Rayleigh-faded IQ time series (see Section VI for details). The blue trace in Fig. 3(a)-(d) is the Rayleigh-faded envelope generated by the simulator. Three rectangular averaging windows, with widths ranging from 0.25λ to 60λ, were applied to the envelope. The red traces are averaged results.

As the window width increases, the variations in the averaged results decrease as is expected. The averaging process transforms the fast-fading time series governed by the Rayleigh probability density function (PDF) into a more slowly varying time-series governed by a different PDF. Fig. 4 shows probability density histograms of the voltage envelope with no averaging, and window widths of 2L = 0.25λ, 1.0λ, and 60λ. A Rayleigh PDF is seen in Fig. 4(a) with no averaging. As the window width increases beyond one wavelength, the resulting voltage envelope distributions become more centered and symmetric. The spread of the resulting distributions also decreases, due to the higher degree of averaging.

For the range of window widths that are typically used in practical mobile channel measurements (20λ-70 λ), the resulting distribution is normal. This can be inferred by applying the Central Limit Theorem to a sum of random variables [4],[6].

III. VARIANCE OF A CONTINUOUS WINDOWED AVERAGE

The variance of the average is used to evaluate the spread in data. It is given by

$$\sigma_{\hat{m}}^2 = \langle \hat{m}^2(x) \rangle - \langle \hat{m}(x) \rangle^2, \tag{10}$$

where $\hat{m}(x)$ is the continuous average (2). The mean square of the estimate $\langle \hat{m}^2(x) \rangle$ is

$$\langle \hat{m}^2(x) \rangle = \frac{1}{4L^2} \int_{x-L}^{x+L} \int_{x-L}^{x+L} \langle r(y_1) r(y_2) \rangle dy_1 dy_2 \,. \tag{11}$$

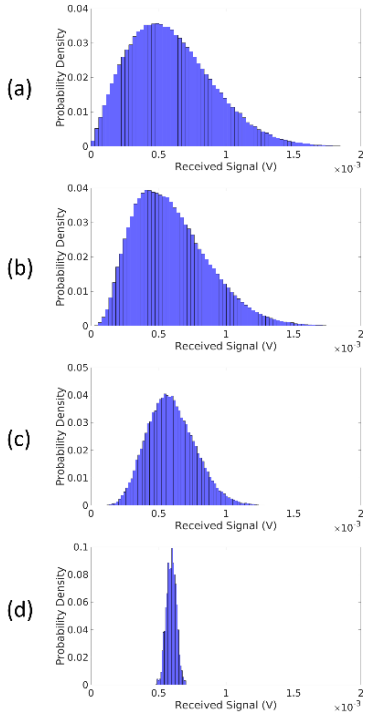

Fig. 4. Histograms of a window-averaged Rayleigh-faded IQ envelope with averaging window widths: (a) No averaging, (b) 2L=0.25λ, (c) 2L=1λ, and (d) 2L=60λ.

Applying (11) and (6) to (10) yields

$$\sigma_{\hat{m}}^2 = \frac{1}{4L^2} \int_{x-L}^{x+L} \int_{x-L}^{x+L} \left[\langle r(y_1) r(y_2) \rangle - \frac{\pi}{2} b^2 \right] dy_1 dy_2 \,. \tag{12}$$

Applying a result from [6] and [7], (12) simplifies to

$$\sigma_{\hat{m}}^2 = \frac{1}{L} \int_0^{2L} \left(1 - \frac{y}{2L}\right) \left[R_r(y) - \frac{\pi}{2} b^2 \right] dy, \tag{13}$$

where $R_r(y)$ is autocorrelation function of the voltage envelope. If a Jakes channel [3] is assumed, the autocorrelation function is given by

$$R_r(y) = \left[\frac{\pi}{4} + \left(1 - \frac{\pi}{4}\right) J_0^2 \left(\frac{2\pi y}{\lambda} \right) \right] 2b^2 \,, \tag{14}$$

where J_o is a zeroth order Bessel function of the first kind, b is the parameter of the Rayleigh distribution in (3), and λ is the wavelength. Substituting (14) into (13) and simplifying yields the result

$$\sigma_{\hat{m}}^2 = \frac{2b^2}{\frac{L}{\lambda}} \left(1 - \frac{\pi}{4}\right) \int_0^{\frac{2L}{\lambda}} \left(1 - \frac{x}{\frac{2L}{\lambda}}\right) J_0^2(2\pi x) dx \,. \tag{15}$$

Lee [8] used the same assumptions used in (11) for his analysis, but obtained the erroneous result

$$\sigma_{\hat{m}}^2 = \frac{\sqrt{\frac{\pi}{2}} b}{2\left(\frac{2L}{\lambda}\right)} \int_0^{\frac{2L}{\lambda}} \left(1 - \frac{x}{\frac{2L}{\lambda}}\right) J_0^2(2\pi x) dx \,. \tag{16}$$

Eq. (15) and (16) contain the same integrals, but the multiplying factors differ. The variance $\sigma_{\hat{m}}^2$ should be proportional to b^2, which is the case for our result (15). Lee's result, therefore, is inconsistent since $\sigma_{\hat{m}}^2$ is proportional to b, and it is incorrect. A direct comparison of (15) and (16), along with validation results, are presented in Section VI.

IV. VARIANCE OF A DISCRETE-TIME WINDOWED AVERAGE

In current propagation measurements, local mean voltage is generally estimated by averaging a finite number of discrete samples. We derive an expression for the variance of the estimated local mean using discrete samples, in analogy to what we did for the case of continuous averaging.

Applying (8) to (10) yields the expression for the variance of the discrete case

$$\sigma_{\hat{m}}^2 = \frac{1}{N^2}\left(\left\langle \left(\sum_{i=1}^{N} r_i \right)^2 \right\rangle - \left(\left\langle \sum_{i=1}^{N} r_i \right\rangle \right)^2 \right)$$
$$= \frac{1}{N}\langle r_i^2 \rangle - \frac{1}{N} m_r^2 + \frac{1}{N^2}\left(\sum_{i=1}^{N}\sum_{j=1}^{N} (1-\delta_{i,j}) \left(\langle r_i r_j \rangle - m_r^2 \right) \right)$$
$$= \frac{\sigma_r^2}{N} + \frac{1}{N^2}\left(\sum_{i=1}^{N}\sum_{j=1}^{N} (1-\delta_{i,j}) \left(\langle r_i r_j \rangle - m_r^2 \right) \right), \qquad (17)$$

where $\delta_{i,j}$ is a Kronecker delta function.

The expression $(\langle r_i r_j \rangle - m_r^2)$ is the covariance of the voltage envelope, which is well-known to be [3]

$$\langle r_i r_j \rangle - m_r^2 = \sigma_r^2 J_0^2 \left(\frac{2\pi (x_i - x_j)}{\lambda} \right) \qquad (18)$$

for the Jake's channel. Since the covariance depends upon $|x_i - x_j|$, the double sum in (17) can be simplified as

$$\sum_{i=1}^{N}\sum_{j=1}^{N} (1-\delta_{i,j}) J_0^2 \left(\frac{2\pi (x_i - x_j)}{\lambda} \right) = 2\sum_{n=1}^{N-1} (N-n)\, J_0^2 \left(\frac{2\pi n d}{\lambda} \right). \qquad (19)$$

This simplification of the double sum to a single sum is analogous to the conversion of the double integral in (12) to the single integral in (13). Substituting (19) into (17), the final expression for the variance is

$$\sigma_{\hat{m}}^2 = \frac{\sigma_r^2}{N}\left[1 + \frac{2}{N}\sum_{n=1}^{N-1} (N-n) J_0^2 \left(\frac{2\pi n d}{\lambda} \right) \right] = \sigma_{uncorr}^2 + \sigma_{corr}^2 \ . \qquad (20)$$

Eq. (20) is analogous to the continuous-average result (15). The first term on the right-hand side of (20) is the usual expression for the variance σ_{uncorr}^2 of the mean obtained by averaging N uncorrelated samples. The sum of Bessel functions is a correction that takes into account correlations among the samples, and is denoted by σ_{corr}^2 .

V. EXPERIMENTAL VERIFICATION

In order to verify the corrected result (15), we performed an experiment using the benchtop setup shown in Fig. 5. The test setup consisted of a channel simulator, vector signal analyzer (VSA), and a laptop computer. The channel simulator generates a CW signal at a user-selected frequency, and it modulates the signal to emulate Rayleigh fading in a NLOS mobile channel. The VSA captures the channel simulator signal and down converts it to a data stream of baseband complex IQ samples. The VSA data is then transferred to a laptop computer for post processing and analysis. A more detailed description of this setup is provided in [1].

The channel simulator was configured to operate at 430 MHz at a power level of -50 dBm and a constant speed of 30 mph (13.4 m/s) with Rayleigh fading. The VSA was configured to capture IQ samples at a rate of 1,284 samples/s. The VSA recorded a continuous record for a period of 15 hours. A record of this length was necessary to provide enough uncorrelated samples for a high-accuracy verification. The recorded time series was first converted to a distance series using the speed-time relation

$$d = v\, t\,, \qquad (21)$$

where d is the distance travelled in meters and v is the velocity in m/s (in this case, 13.4 m/s). We chose a 13.4 m/s for our simulator, since this is a typical speed for drive tests in urban areas.

The transformed record was then segmented in time into a sequence of P contiguous blocks, each of width of $2L$, as is shown in Fig. 6. We set the number of blocks at $P = 17{,}300$ throughout the analysis to provide both high accuracy and a constant number of terms as a baseline. We used 12 different block widths of $2L$ that ranged from a minimum of 5λ to a maximum of 60λ. For each case, we computed the mean value for each data block to obtain a sequence of sample means given by m_i^{blk} $(i = 1,2,\ldots P)$ where the superscript "blk" denotes a data block within the ensemble of averages.

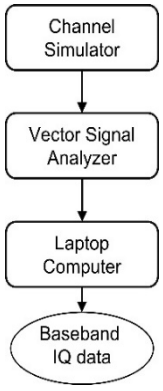

Fig. 5. Block diagram of the benchtop setup for the experimental verification.

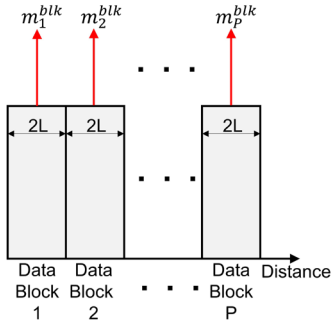

Fig. 6. Segmenting the simulator IQ envelope data into P contiguous blocks of width $2L$. $P = 17{,}300$ for the analysis.

The resulting sequence is first used to compute sample mean given by

$$m^s = \frac{1}{P}\sum_{i=1}^{P} m_i^{blk} \,. \qquad (22)$$

The sample standard deviation of block averages is then evaluated to yield

$$s^s = \sqrt{\frac{1}{(P-1)}\sum_{i=1}^{P}(m_i^{blk} - m^s)^2} \,. \qquad (23)$$

The selection of contiguous data blocks of width 2L results in a sequence with weakly correlated mean values.

Fig. 7 shows a direct comparison of the experimental results obtained from both (15) and (16), with the Rayleigh PDF parameter of the governing distribution set to b=1. The experimental data was normalized to obtain a Rayleigh PDF parameter b=1. The experimental data closely agrees with the new corrected result (15). Lee's formula (16) exhibits a noticeable offset which is due to the error in the multiplying factor.

In order to quantify variations (in dB) about a local mean at a location x, Lee [8] defines the so-called "2 $\sigma_{\hat{m}}$ spread" (in dB) as

$$2\,\sigma_{\hat{m}}\; spread = 20\,log_{10}\frac{m_r + \sigma_{\hat{m}}}{m_r - \sigma_{\hat{m}}} \quad (dB), \qquad (24)$$

where m_r is the mean given in (9), and $\sigma_{\hat{m}}$ is the standard deviation derived from either (15) or (16). Fig. 8 shows three curves with the Rayleigh parameter set at b = 1. The red trace is the corrected result (15). The blue trace is Lee's result (16). The "+" tick marks are obtained from (24) using experimental data in conjunction with (22) and (23). Close agreement is seen with results obtained from (15). A spread of 1 dB is seen at $2L$ = 60λ. Lee's variance (16) generates a 2 $\sigma_{\hat{m}}$ $spread$ spread of 1 dB for $2L$ = 40λ. Thus, the 40λ criteria, which is one of the primary claims of [8] and widely cited, should be corrected to $2L$ = 60λ.

VI. CONTINUOUS AND DISCRETE AVERAGING COMPARED

So far, we have developed analytical expressions for the variances encountered in continuous and discrete window averaging. A question that arises is how do these two types of averaging compare? We performed a direct intercomparison by applying windows to a fading-simulator-generated IQ time series. Fig. 9 shows a comparison of standard deviations obtained from the continuous window average (red trace) to those obtained as a function of discrete averaging as depicted in Fig. 2.

The red trace is the continuous average for a fixed window width of 60λ. The blue trace depicts the discrete averages. The overall window width is fixed at 60λ, and the sample spacings are computed from (7) by varying the number of samples N over the range 13 ≤ N ≤ 241. The range of the resulting sample spacings is 0.25λ ≤ λ ≤ 5λ.

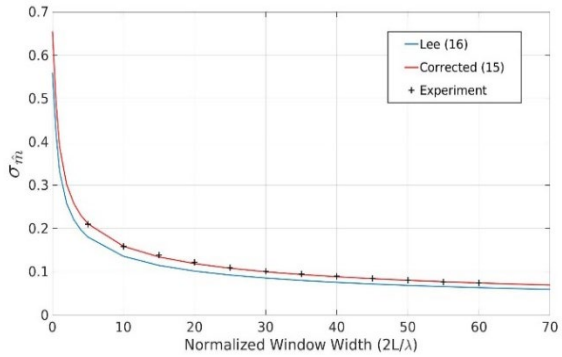

Fig. 7. A comparison of the estimated local mean variances obtained from the corrected result (15) (red trace), Lee (16) (blue trace), and channel simulator measurements (+ tick marks).

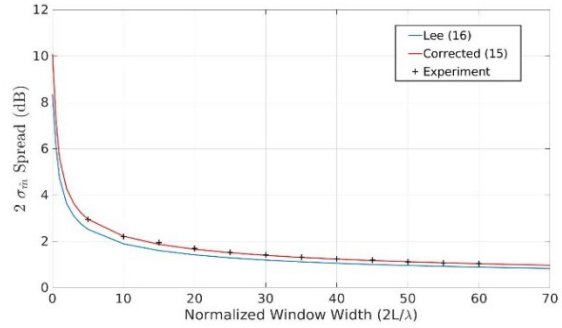

Fig. 8. A comparison of the estimated **2 $\sigma_{\hat{m}}$** spread obtained from the corrected result (15) (red trace), Lee (16) (blue trace), and channel simulator measurements ("+" tick marks).

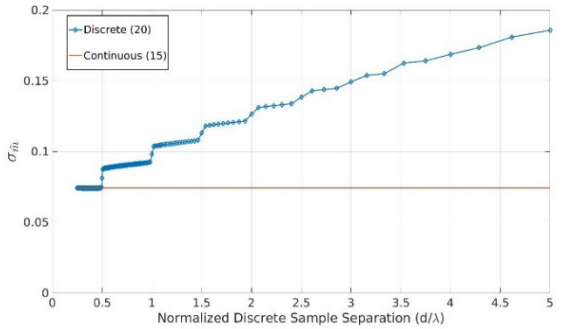

Fig. 9. Standard deviation of discrete window averages as a function of sample spacing (blue trace) for a window width of $2L$ = 60λ. The red trace is the continuous window result.

The discrete results are plotted as blue diamond tick marks and interconnecting lines. As the sample spacing decreases, the resulting standard deviations are reduced. Close agreement is observed with the continuous case for d < 0.5λ. A distinct "staircase effect" is seen in the discrete case for d < 3λ. This is due to the series of Bessel functions on the right-hand side of (20) which become more oscillatory as the spacing decreases and the samples rapidly become more correlated. Although not shown here, we performed similar comparisons for averaging window widths of 5λ, 10λ, 20λ, 40λ, and 100λ.

In all cases, the same general characteristics are seen. First, close agreement occurs with d < 0.5λ for continuous and discrete windows, yielding virtually identical averages and variances for

sample spacing less than 0.5λ. This makes sense given that the sum in (8) closely approximates the integral in (2) as the number of samples becomes large.

In order to better understand the impact of the series term on the right side of (20), the following ratio provides a useful metric

$$P_{rat} = \frac{\sigma^2_{corr}}{\sigma^2_{uncorr}}, \qquad (25)$$

where σ^2_{uncorr} is the uncorrelated term in (20) and σ^2_{uncorr} is the sum of Bessel functions that accounts for the correlation between the samples. Eq. (25) provides a direct metric of the correlatedness in (20).

Fig. 10 shows P_{rat} obtained with an averaging window width of 60λ and sample spacings ranging from 0.25λ to 5λ. As the sample spacing increases beyond 2λ, the fraction of variance contributed by the series in (20) decreases below 0.2, and the samples are weakly correlated. For separations less than 2λ, P_{rat} rapidly increases as the samples become more correlated. A "staircasing" effect is seen in the results once again, due to oscillations in the Bessel functions. The Bessel function series becomes dominant with d < 0.5 λ.

We performed further analyses at window widths of 20λ, 40λ, and 100λ and similar trends were seen. Some variability is seen for the sample spacing for which $P_{rat} < 0.2$. The sample spacings for which this condition was met occurred for $2\lambda < L < 3.5\,\lambda$. A rapid increase in P_{rat} is always seen with $d < 0.5\,\lambda$. Pronounced "staircasing" occurs for sample spacing $d < 2\,\lambda$.

VII. Conclusions

We have presented an analysis of both continuous and discrete window averaging in a NLOS Rayleigh fast-fading channel. An updated result for the variance of a continuous averaging window is given, along with an associated $2\,\sigma_{\widehat{m}}$ spread. Our results correct an error in the variance derived by Lee [8]. Our correction to variance results in a $2L = 60\lambda$ averaging length to achieve a 1 dB $2\,\sigma_{\widehat{m}}$ spread. Lee originally predicted a $2L = 40\lambda$ to achieve a 1 dB spread.

We have also developed a new and highly useful variance expression for an averaging window that uses uniformly spaced discrete sampling with a separation *d*. For a sample spacing of $d < 0.5\lambda$ our analysis shows that discrete sampling is virtually identical to continuous averaging for window widths $5\lambda \le 2L \le 100\lambda$. Our results also show a rapid increase in the amount of correlation between samples for spacings of less than 2λ. As the sample spacing is increased beyond 3λ, the samples are weakly correlated—the variance (20) is well approximated by uncorrelated samples. We have derived a new and significant result for discrete sampling that modifies the established independence criteria for channel sample spacing in a Rayleigh NLOS channel.

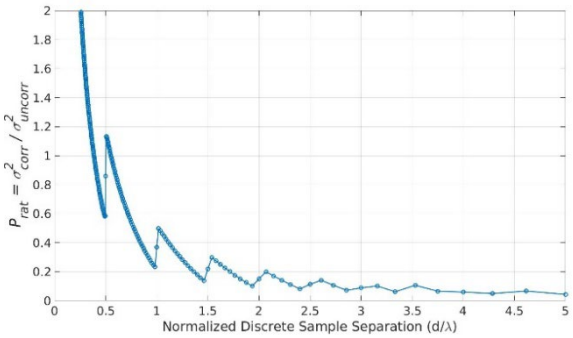

Fig. 10. The fractional contribution of the Bessel function series in (20) to the overall variance for a discrete averaging window of width $2L = 60\lambda$.

Acknowledgment

The authors thank Dr. Roger Dalke, formerly with ITS, for his assistance in simplifying the variance expressions and many helpful and illuminating discussions about fast-fading mobile channels.

References

[1] Robert Johnk, Chriss Hammerschmidt, Irena Stange, "A high-performance CW Channel Sounder," *IEEE Int. Symp. EMC and Signal/Power Integrity*, Aug, 7-11, 2017, pp. 698-703.

[2] Chriss Hammerschmidt and Robert Johnk, "Extracting clutter metrics in the 1755-1780 MHz band, *Proc. of the IEEE Military Communications Conf.*, Baltimore, MD, Nov. 1-3, 2016.

[3] W.C. Jakes, Ed., *Microwave Mobile Communications*, IEEE, Inc., New York, 1994, p.38

[4] Steven Kay, *Intuitive Probability and Random Processes using MATLAB®*, Springer, New York, New York, 2006.

[5] J. D. Parsons, *The Mobile Radio Propagation Channel*, John Wiley & Sons, New York, New York, 2000.

[6] A. Papoulis, *Probability, Random Variables, and Stochastic Processes*, McGraw-Hill, New York, 1965, p. 325.

[7] Garry C. Hess, *Handbook of Land-Mobile Radio Radio System Coverage*, Artech House, Norwood MA, 1998, Chapter 3.

[8] W.C.Y. Lee, "Estimate of local average power of a mobile radio signal," *IEEE Trans. Vehicular Tech.*, VT-34,no. 1, Feb 1985.